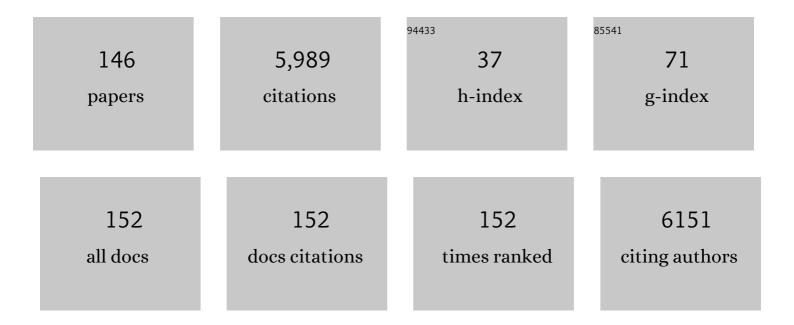
List of Publications by Year in descending order

Source: https://exaly.com/author-pdf/3395099/publications.pdf Version: 2024-02-01



NEIL VASDEV

#	Article	lF	CITATIONS
1	Tau positron emission tomographic imaging in aging and early <scp>A</scp> lzheimer disease. Annals of Neurology, 2016, 79, 110-119.	5.3	778
2	Validating novel tau positron emission tomography tracer <scp>[Fâ€18]â€AVâ€1451 (T807)</scp> on postmortem brain tissue. Annals of Neurology, 2015, 78, 787-800.	5.3	535
3	Chemistry for Positron Emission Tomography: Recent Advances in ¹¹ Câ€; ¹⁸ Fâ€; ¹³ Nâ€; and ¹⁵ Oâ€Labeling Reactions. Angewandte Chemie - International Edition, 2019, 58, 2580-2605.	13.8	216
4	Spirocyclic hypervalent iodine(III)-mediated radiofluorination of non-activated and hindered aromatics. Nature Communications, 2014, 5, 4365.	12.8	207
5	Tau Positron Emission Tomographic Imaging in the Lewy Body Diseases. JAMA Neurology, 2016, 73, 1334.	9.0	182
6	Radiosynthesis and initial evaluation of [18F]-FEPPA for PET imaging of peripheral benzodiazepine receptors. Nuclear Medicine and Biology, 2008, 35, 305-314.	0.6	181
7	Emerging PET Radiotracers and Targets for Imaging of Neuroinflammation in Neurodegenerative Diseases: Outlook Beyond TSPO. Molecular Imaging, 2018, 17, 153601211879231.	1.4	158
8	Chelate-free metal ion binding and heat-induced radiolabeling of iron oxide nanoparticles. Chemical Science, 2015, 6, 225-236.	7.4	107
9	Mechanistic studies and radiofluorination of structurally diverse pharmaceuticals with spirocyclic iodonium(<scp>iii</scp>) ylides. Chemical Science, 2016, 7, 4407-4417.	7.4	104
10	¹¹ Cî€O bonds made easily for positron emission tomography radiopharmaceuticals. Chemical Society Reviews, 2016, 45, 4708-4726.	38.1	98
11	11CO2 fixation: a renaissance in PET radiochemistry. Chemical Communications, 2013, 49, 5621.	4.1	92
12	Sifting through the surfeit of neuroinflammation tracers. Journal of Cerebral Blood Flow and Metabolism, 2018, 38, 204-224.	4.3	92
13	Kinetic Modeling of the Monoamine Oxidase B Radioligand [¹¹ C]SL25.1188 in Human Brain with High-Resolution Positron Emission Tomography. Journal of Cerebral Blood Flow and Metabolism, 2014, 34, 883-889.	4.3	83
14	Recent developments on PET radiotracers for TSPO and their applications in neuroimaging. Acta Pharmaceutica Sinica B, 2021, 11, 373-393.	12.0	82
15	[11C]CURB: Evaluation of a novel radiotracer for imaging fatty acid amide hydrolase by positron emission tomography. Nuclear Medicine and Biology, 2011, 38, 247-253.	0.6	76
16	¹⁸ F‣abeling of Sensitive Biomolecules for Positron Emission Tomography. Chemistry - A European Journal, 2017, 23, 15553-15577.	3.3	75
17	Monoamine Oxidase B Total Distribution Volume in the Prefrontal Cortex of Major Depressive Disorder. JAMA Psychiatry, 2019, 76, 634.	11.0	74
18	Synthesis and Application of Isocyanates Radiolabeled with Carbonâ€11. Chemistry - A European Journal, 2011, 17, 259-264.	3.3	73

#	Article	IF	CITATIONS
19	Pharmacokinetic Evaluation of the Tau PET Radiotracer ¹⁸ F-T807 (¹⁸ F-AV-1451) in Human Subjects. Journal of Nuclear Medicine, 2017, 58, 484-491.	5.0	73
20	A concise radiosynthesis of the tau radiopharmaceutical, [¹⁸ F]T807. Journal of Labelled Compounds and Radiopharmaceuticals, 2013, 56, 736-740.	1.0	70
21	Discovery of a Highly Selective Glycogen Synthase Kinaseâ€3 Inhibitor (PFâ€04802367) That Modulates Tau Phosphorylation in the Brain: Translation for PET Neuroimaging. Angewandte Chemie - International Edition, 2016, 55, 9601-9605.	13.8	68
22	Radiosynthesis of [¹¹ C]SL25.1188 via [¹¹ C]CO ₂ fixation for imaging monoamine oxidase B. Journal of Labelled Compounds and Radiopharmaceuticals, 2011, 54, 678-680.	1.0	67
23	lodonium Ylide–Mediated Radiofluorination of ¹⁸ F-FPEB and Validation for Human Use. Journal of Nuclear Medicine, 2015, 56, 489-492.	5.0	65
24	Direct fixation of [¹¹ C]-CO ₂ by amines: formation of [¹¹ C-carbonyl]-methylcarbamates. Organic and Biomolecular Chemistry, 2010, 8, 428-432.	2.8	64
25	<i>Ortho</i> tabilized ¹⁸ Fâ€Azido Click Agents and their Application in PET Imaging with Single‧tranded DNA Aptamers. Angewandte Chemie - International Edition, 2015, 54, 12777-12781.	13.8	62
26	¹⁸ F-Labeled Single-Stranded DNA Aptamer for PET Imaging of Protein Tyrosine Kinase-7 Expression. Journal of Nuclear Medicine, 2015, 56, 1780-1785.	5.0	59
27	Synthesis and ex vivo evaluation of carbon-11 labelled N-(4-methoxybenzyl)-N′-(5-nitro-1,3-thiazol-2-yl)urea ([11C]AR-A014418): A radiolabelled glycogen synthase kinase-3β specific inhibitor for PET studies. Bioorganic and Medicinal Chemistry Letters, 2005, 15, 5270-5273.	2.2	57
28	Radiolabeled Small Molecule Protein Kinase Inhibitors for Imaging with PET or SPECT. Molecules, 2010, 15, 8260-8278.	3.8	53
29	Synthesis and Preclinical Evaluation of Sulfonamido-based [¹¹ C- <i>Carbonyl</i>]-Carbamates and Ureas for Imaging Monoacylglycerol Lipase. Theranostics, 2016, 6, 1145-1159.	10.0	50
30	Recent Advances in ¹⁸ F Radiochemistry: A Focus on B- ¹⁸ F, Si- ¹⁸ F, Al- ¹⁸ F, and C- ¹⁸ F Radiofluorination via Spirocyclic Iodonium Ylides. Journal of Nuclear Medicine, 2018, 59, 568-572.	5.0	50
31	A Facile Radiolabeling of [¹⁸ F]FDPA via Spirocyclic Iodonium Ylides: Preliminary PET Imaging Studies in Preclinical Models of Neuroinflammation. Journal of Medicinal Chemistry, 2017, 60, 5222-5227.	6.4	43
32	On the consensus nomenclature rules for radiopharmaceutical chemistry – Reconsideration of radiochemical conversion. Nuclear Medicine and Biology, 2021, 93, 19-21.	0.6	43
33	Radiosynthesis and Evaluation of [¹¹ C- <i>Carbonyl</i>]-Labeled Carbamates as Fatty Acid Amide Hydrolase Radiotracers for Positron Emission Tomography. Journal of Medicinal Chemistry, 2013, 56, 201-209.	6.4	42
34	Enzymeâ€Mediated Modification of Singleâ€Domain Antibodies for Imaging Modalities with Different Characteristics. Angewandte Chemie - International Edition, 2016, 55, 528-533.	13.8	42
35	Classics in Neuroimaging: Development of PET Tracers for Imaging Monoamine Oxidases. ACS Chemical Neuroscience, 2019, 10, 1867-1871.	3.5	42
36	Novel Fluorinated 8-Hydroxyquinoline Based Metal Ionophores for Exploring the Metal Hypothesis of Alzheimer's Disease. ACS Medicinal Chemistry Letters, 2015, 6, 1025-1029.	2.8	41

NEIL VASDEV

#	Article	IF	CITATIONS
37	[¹¹ C]Cyanation of arylboronic acids in aqueous solutions. Chemical Communications, 2017, 53, 6597-6600.	4.1	41
38	In Vitro and in Vivo Evaluation of ¹¹ C-Labeled Azetidinecarboxylates for Imaging Monoacylglycerol Lipase by PET Imaging Studies. Journal of Medicinal Chemistry, 2018, 61, 2278-2291.	6.4	41
39	Development of new radiopharmaceuticals for imaging monoamine oxidase B. Nuclear Medicine and Biology, 2011, 38, 933-943.	0.6	40
40	Alternative approaches for PET radiotracer development in Alzheimer's disease: imaging beyond plaque. Journal of Labelled Compounds and Radiopharmaceuticals, 2014, 57, 323-331.	1.0	39
41	Synthesis of [¹¹ C]Bexarotene by Cu-Mediated [¹¹ C]Carbon Dioxide Fixation and Preliminary PET Imaging. ACS Medicinal Chemistry Letters, 2014, 5, 668-672.	2.8	39
42	Synthesis of ¹⁸ Fâ€Difluoromethylarenes from Aryl (Pseudo) Halides. Angewandte Chemie - International Edition, 2016, 55, 10786-10790.	13.8	38
43	Microfluidic continuous-flow radiosynthesis of [¹⁸ F]FPEB suitable for human PET imaging. MedChemComm, 2014, 5, 432-435.	3.4	37
44	Radiosynthesis and ex vivo evaluation of [11C-carbonyl]carbamate- and urea-based monoacylglycerol lipase inhibitors. Nuclear Medicine and Biology, 2014, 41, 688-694.	0.6	34
45	Towards the preparation of radiolabeled 1-aryl-3-benzyl ureas: Radiosynthesis of [11C-carbonyl] AR-A014418 by [11C]CO2 fixation. Bioorganic and Medicinal Chemistry Letters, 2012, 22, 2099-2101.	2.2	33
46	Positron Emission Tomography Imaging of the Endocannabinoid System: Opportunities and Challenges in Radiotracer Development. Journal of Medicinal Chemistry, 2021, 64, 123-149.	6.4	33
47	First Human Use of a Radiopharmaceutical Prepared by Continuous-Flow Microfluidic Radiofluorination: Proof of Concept with the Tau Imaging Agent [¹⁸ F]T807. Molecular Imaging, 2014, 13, 7290.2014.00025.	1.4	32
48	Pharmacodynamic Imaging Guides Dosing of a Selective Estrogen Receptor Degrader. Clinical Cancer Research, 2015, 21, 1340-1347.	7.0	32
49	Translocator Protein Distribution Volume Predicts Reduction of Symptoms During Open-Label Trial of Celecoxib in Major Depressive Disorder. Biological Psychiatry, 2020, 88, 649-656.	1.3	32
50	Utility of commercial radiosynthetic modules in captive solvent [¹¹ C]â€methylation reactions. Journal of Labelled Compounds and Radiopharmaceuticals, 2009, 52, 490-492.	1.0	31
51	Structural Basis for Achieving GSK-3Î ² Inhibition with High Potency, Selectivity, and Brain Exposure for Positron Emission Tomography Imaging and Drug Discovery. Journal of Medicinal Chemistry, 2019, 62, 9600-9617.	6.4	31
52	Chemie der Positronenemissionstomographie: Aktuelle Fortschritte bei ¹¹ Câ€, ¹⁸ Fâ€, ¹³ N―und ¹⁵ Oâ€Markierungsreaktionen. Angewandte Chemie, 2 131, 2604-2631.	20229	31
53	Rapid microfluidic flow hydrogenation for reduction or deprotection of 18F-labeled compounds. Chemical Communications, 2013, 49, 8755.	4.1	30
54	Alantolactone selectively ablates acute myeloid leukemia stem and progenitor cells. Journal of Hematology and Oncology, 2016, 9, 93.	17.0	30

NEIL VASDEV

#	Article	IF	CITATIONS
55	Synthesis and PET imaging studies of [18F]2-fluoroquinolin-8-ol ([18F]CABS13) in transgenic mouse models of Alzheimer's disease. MedChemComm, 2012, 3, 1228.	3.4	29
56	Development and characterization of a promising fluorine-18 labelled radiopharmaceutical for in vivo imaging of fatty acid amide hydrolase. Bioorganic and Medicinal Chemistry, 2013, 21, 4351-4357.	3.0	29
57	Radiosynthesis, <i>In Vitro</i> and <i>In Vivo</i> Evaluation of [¹⁸ F]CBD-2115 as a First-in-Class Radiotracer for Imaging 4R-Tauopathies. ACS Chemical Neuroscience, 2021, 12, 596-602.	3.5	29
58	On The Preparation of Fluorine-18 Labelled XeF2and Chemical Exchange between Fluoride Ion and XeF2. Journal of the American Chemical Society, 2002, 124, 12863-12868.	13.7	28
59	Synthesis and preclinical evaluation of [11C-carbonyl]PF-04457845 for neuroimaging of fatty acid amide hydrolase. Nuclear Medicine and Biology, 2013, 40, 740-746.	0.6	28
60	Design, Synthesis, and Evaluation of Reversible and Irreversible Monoacylglycerol Lipase Positron Emission Tomography (PET) Tracers Using a "Tail Switching―Strategy on a Piperazinyl Azetidine Skeleton. Journal of Medicinal Chemistry, 2019, 62, 3336-3353.	6.4	28
61	cGMP production of the radiopharmaceutical [¹⁸ F]MK-6240 for PET imaging of human neurofibrillary tangles. Journal of Labelled Compounds and Radiopharmaceuticals, 2017, 60, 263-269.	1.0	27
62	Improving PET Imaging Acquisition and Analysis With Machine Learning: A Narrative Review With Focus on Alzheimer's Disease and Oncology. Molecular Imaging, 2019, 18, 153601211986907.	1.4	27
63	Facile 18F labeling of non-activated arenes via a spirocyclic iodonium(III) ylide method and its application in the synthesis of the mGluR5 PET radiopharmaceutical [18F]FPEB. Nature Protocols, 2019, 14, 1530-1545.	12.0	27
64	Development of new carbon-11 labelled radiotracers for imaging GABAA- and GABAB-benzodiazepine receptors. Bioorganic and Medicinal Chemistry, 2012, 20, 4482-4488.	3.0	25
65	Total Radiosynthesis: Thinking Outside â€~the Box'. Australian Journal of Chemistry, 2015, 68, 1319.	0.9	25
66	Syntheses and in vitro evaluation of fluorinated naphthoxazines as dopamine D2/D3 receptor agonists: radiosynthesis, ex vivo biodistribution and autoradiography of [18F]F-PHNO. Nuclear Medicine and Biology, 2007, 34, 195-203.	0.6	24
67	Metal-free ¹⁸ F-labeling of aryl-CF ₂ H via nucleophilic radiofluorination and oxidative C–H activation. Chemical Communications, 2017, 53, 126-129.	4.1	24
68	PET Neuroimaging Studies of [¹⁸ F]CABS13 in a Double Transgenic Mouse Model of Alzheimer's Disease and Nonhuman Primates. ACS Chemical Neuroscience, 2015, 6, 535-541.	3.5	23
69	"Inâ€loop―[¹¹ C]CO ₂ fixation: Prototype and proof of concept. Journal of Labelled Compounds and Radiopharmaceuticals, 2018, 61, 252-262.	1.0	23
70	Development of [¹⁸ F]Maleimide-Based Glycogen Synthase Kinase-3β Ligands for Positron Emission Tomography Imaging. ACS Medicinal Chemistry Letters, 2017, 8, 287-292.	2.8	22
71	Selected PET Radioligands for Ion Channel Linked Neuroreceptor Imaging: Focus on GABA, NMDA and nACh Receptors. Current Topics in Medicinal Chemistry, 2016, 16, 1830-1842.	2.1	22
72	[18F]Fluoroamines via ring-opening of N-Cbz-2-methylaziridine with [18F]-fluoride. Tetrahedron Letters, 2009, 50, 544-547.	1.4	21

#	Article	IF	CITATIONS
73	Brain Penetration of the ROS1/ALK Inhibitor Lorlatinib Confirmed by PET. Molecular Imaging, 2017, 16, 153601211773666.	1.4	21
74	An improved radiosynthesis of the muscarinic M2 radiopharmaceutical, [18F]FP-TZTP. Applied Radiation and Isotopes, 2009, 67, 611-616.	1.5	20
75	Synthesis of 18F-arenes from spirocyclic iodonium(III) ylides via continuous-flow microfluidics. Journal of Fluorine Chemistry, 2015, 178, 249-253.	1.7	20
76	<i>In Vitro</i> Evaluation of [³ H]CPPC as a Tool Radioligand for CSF-1R. ACS Chemical Neuroscience, 2021, 12, 998-1006.	3.5	19
77	PET radiopharmaceuticals for probing enzymes in the brain. American Journal of Nuclear Medicine and Molecular Imaging, 2013, 3, 194-216.	1.0	19
78	PET Imaging of Fatty Acid Amide Hydrolase with [¹⁸ F]DOPP in Nonhuman Primates. Molecular Pharmaceutics, 2014, 11, 3832-3838.	4.6	18
79	Evaluating the accuracy of density functional theory for calculating 1H and 13C NMR chemical shifts in drug molecules. Computational and Theoretical Chemistry, 2015, 1051, 161-172.	2.5	18
80	Cognitive impairment and World Trade Centre-related exposures. Nature Reviews Neurology, 2022, 18, 103-116.	10.1	18
81	Synthesis and preliminary biological evaluations of [18F]-1-deoxy-1-fluoro-scyllo-inositol. Chemical Communications, 2009, , 5527.	4.1	17
82	NMR Spectroscopic Evidence for the Intermediacy of XeF ₃ ^{â^'} in XeF ₂ /F ^{â^'} Exchange, Attempted Syntheses and Thermochemistry of XeF ₃ ^{â^'} Salts, and Theoretical Studies of the XeF ₃ ^{â^'} Anion. Inorganic Chemistry, 2010, 49, 8997-9004.	4.0	17
83	Synthesis and Preliminary PET Imaging Studies of a FAAH Radiotracer ([¹¹ C]MPPO) Based on α-Ketoheterocyclic Scaffold. ACS Chemical Neuroscience, 2016, 7, 109-118.	3.5	17
84	Regioselective ring opening of 2-methylaziridine derivatives with 18F- and 19F-fluoride. Tetrahedron Letters, 2011, 52, 4114-4116.	1.4	16
85	Radiosynthesis and preliminary PET evaluation of 18 F-labeled 2-(1-(3-fluorophenyl)-2-oxo-5-(pyrimidin-2-yl)-1,2-dihydropyridin-3-yl)benzonitrile for imaging AMPA receptors. Bioorganic and Medicinal Chemistry Letters, 2016, 26, 4857-4860.	2.2	16
86	Imaging of astrocytes in posttraumatic stress disorder: A PET study with the monoamine oxidase B radioligand [11C]SL25.1188. European Neuropsychopharmacology, 2022, 54, 54-61.	0.7	16
87	Comparisons of [18F]-1-deoxy-1-fluoro-scyllo-inositol with [18F]-FDG for PET imaging of inflammation, breast and brain cancer xenografts in athymic mice. Nuclear Medicine and Biology, 2011, 38, 953-959.	0.6	15
88	Radiosynthesis and ex vivo evaluation of [18F]-(S)-3-(6-(3-fluoropropoxy)benzo[d]isoxazol-3-yl)-5-(methoxymethyl)oxazolidin-2-one for imaging MAO-B with PET. Bioorganic and Medicinal Chemistry Letters, 2015, 25, 288-291.	2.2	15
89	Classics in Neuroimaging: Imaging the Dopaminergic Pathway with PET. ACS Chemical Neuroscience, 2017, 8, 1817-1819.	3.5	15
90	Synthesis and preclinical evaluation of [18F]FSL25.1188, a reversible PET radioligand for monoamine oxidase-B. Bioorganic and Medicinal Chemistry Letters, 2019, 29, 1624-1627.	2.2	15

#	Article	IF	CITATIONS
91	Radiosynthesis of a Bruton's tyrosine kinase inhibitor, [¹¹ C]Tolebrutinib, via palladiumâ€NiXantphosâ€mediated carbonylation. Journal of Labelled Compounds and Radiopharmaceuticals, 2020, 63, 482-487.	1.0	15
92	Preclinical Evaluation of TSPO and MAO-B PET Radiotracers in an LPS Model of Neuroinflammation. PET Clinics, 2021, 16, 233-247.	3.0	15
93	Discovery of PET radiopharmaceuticals at the academia-industry interface. Drug Discovery Today: Technologies, 2017, 25, 19-26.	4.0	14
94	Copper(I)-Mediated 11C-Carboxylation of (Hetero)arylstannanes. ACS Omega, 2020, 5, 8242-8250.	3.5	14
95	Synthesis and Reactivity of ¹⁸ F-Labeled α,α-Difluoro-α-(aryloxy)acetic Acids. Organic Letters, 2017, 19, 568-571.	4.6	13
96	Classics in Neuroimaging: Imaging the Endocannabinoid Pathway with PET. ACS Chemical Neuroscience, 2020, 11, 1855-1862.	3.5	13
97	The effect of aromatic fluorine substitution in I-DOPA on the in vivo behaviour of []2-, []5- and []6-fluoro-I-DOPA in the human brain. Journal of Fluorine Chemistry, 2002, 115, 33-39.	1.7	12
98	Radiosynthesis, ex vivo and in vivo evaluation of [11C]preclamol as a partial dopamine D2 agonist radioligand for positron emission tomography. Synapse, 2006, 60, 314-318.	1.2	11
99	Stereoselective ¹¹ C Labeling of a "Native―Tetrapeptide by Using Asymmetric Phaseâ€Transfer Catalyzed Alkylation Reactions. European Journal of Organic Chemistry, 2017, 2017, 1019-1024.	2.4	11
100	Metal Protein-Attenuating Compound for PET Neuroimaging: Synthesis and Preclinical Evaluation of [¹¹ C]PBT2. Molecular Pharmaceutics, 2018, 15, 695-702.	4.6	11
101	Revisiting the Radiosynthesis of [18F]FPEB and Preliminary PET Imaging in a Mouse Model of Alzheimer's Disease. Molecules, 2020, 25, 982.	3.8	11
102	Synthesis and preliminary evaluation of [18F]-fluoro-(2S)-Exaprolol for imaging cerebral β-adrenergic receptors with PET. Neurochemistry International, 2008, 53, 173-179.	3.8	10
103	Synthesis and Preclinical Evaluation of [18F]FCHC for Neuroimaging of Fatty Acid Amide Hydrolase. Molecular Imaging and Biology, 2015, 17, 257-263.	2.6	10
104	A Workshop on Cognitive Aging and Impairment in the 9/11-Exposed Population. International Journal of Environmental Research and Public Health, 2021, 18, 681.	2.6	10
105	Target receptor identification and subsequent treatment of resected brain tumors with encapsulated and engineered allogeneic stem cells. Nature Communications, 2022, 13, 2810.	12.8	10
106	Facile Radiosynthesis of Fluorine-18 Labeled Î ² -Blockers. Synthesis, Radiolabeling, and ex Vivo Biodistribution of [¹⁸ F]-(2 <i>S</i> and) Tj ETQq0 0 0 rgBT /Overlock 10 Tf 50 142 Td (2 <i>R</i>)-1-(Chemistry, 2008, 51, 5093-5100.	(1-Fluorop 6.4	propan-2-ylar
107	Classics in Neuroimaging: Development of Positron Emission Tomography Tracers for Imaging the GABAergic Pathway. ACS Chemical Neuroscience, 2020, 11, 2039-2044.	3.5	9
108	Preclinical PET Neuroimaging of [¹¹ C]Bexarotene. Molecular Imaging, 2016, 15,	1.4	8

108 153601211666305.

#	Article	IF	CITATIONS
109	The Search for a Subtype-Selective PET Imaging Agent for the GABA _A Receptor Complex: Evaluation of the Radiotracer [¹¹ C]ADO in Nonhuman Primates. Molecular Imaging, 2017, 16, 153601211773125.	1.4	8
110	Microfluidic radiosynthesis of [¹⁸ F]FEMPT, a high affinity PET radiotracer for imaging serotonin receptors. Beilstein Journal of Organic Chemistry, 2017, 13, 2922-2927.	2.2	8
111	Fluorine-18 labelled Ruppert–Prakash reagent ([¹⁸ F]Me ₃ SiCF ₃) for the synthesis of ¹⁸ F-trifluoromethylated compounds. Chemical Communications, 2021, 57, 5286-5289.	4.1	8
112	Radiofluorination of oxazole-carboxamides for preclinical PET neuroimaging of GSK-3. Journal of Fluorine Chemistry, 2021, 245, 109760.	1.7	8
113	Radiosynthesis of [11C]Ibrutinib via Pd-Mediated [11C]CO Carbonylation: Preliminary PET Imaging in Experimental Autoimmune Encephalomyelitis Mice. Frontiers in Nuclear Medicine, 2021, 1, .	1.2	8
114	The Assay of Enzyme Activity by Positron Emission Tomography. Neuromethods, 2012, , 111-135.	0.3	7
115	"Inâ€loop― ¹⁸ Fâ€fluorination: A proofâ€ofâ€concept study. Journal of Labelled Compounds and Radiopharmaceuticals, 2019, 62, 292-297.	1.0	7
116	Training the next generation of radiopharmaceutical scientists. Nuclear Medicine and Biology, 2020, 88-89, 10-13.	0.6	7
117	In Vitro and In Vivo Evaluation of GSK-3 Radioligands in Alzheimer's Disease: Preliminary Evidence of Sex Differences. ACS Pharmacology and Translational Science, 2021, 4, 1287-1294.	4.9	7
118	Synthesis and in vitro evaluation of derivatives of the β1-adrenergic receptor antagonist HX-CH 44. Bioorganic and Medicinal Chemistry Letters, 2011, 21, 5506-5509.	2.2	6
119	Radiosynthesis and in vivo tumor uptake of 2-deoxy-2-[18F]fluoro-myo-inositol. Bioorganic and Medicinal Chemistry Letters, 2012, 22, 6148-6150.	2.2	6
120	Recent applications of a single quadrupole mass spectrometer in 11C, 18F and radiometal chemistry. Journal of Fluorine Chemistry, 2018, 210, 46-55.	1.7	6
121	Fluorine-18: an untapped resource in inorganic chemistry. Chemical Communications, 2018, 54, 11835-11842.	4.1	6
122	Repurposing ¹¹ C-PS13 for PET Imaging of Cyclooxygenase-1 in Ovarian Cancer Xenograft Mouse Models. Journal of Nuclear Medicine, 2021, 62, 665-668.	5.0	6
123	Artificial intelligence for molecular neuroimaging. Annals of Translational Medicine, 2021, 9, 822-822.	1.7	6
124	Fluorinated Adenosine A2A Receptor Antagonists Inspired by Preladenant as Potential Cancer Immunotherapeutics. International Journal of Medicinal Chemistry, 2017, 2017, 1-8.	2.2	5
125	Leveraging Open Science Drug Development for PET: Preliminary Neuroimaging of ¹¹ C-Labeled ALK2 Inhibitors. ACS Medicinal Chemistry Letters, 2021, 12, 846-850.	2.8	5
126	Synthesis, in vitro and in vivo evaluation of 11C-O-methylated arylpiperazines as potential serotonin 1A (5-HT1A) receptor antagonist radiotracers. EJNMMI Radiopharmacy and Chemistry, 2020, 5, 13.	3.9	5

#	Article	IF	CITATIONS
127	Design and Prototype of an Automated Column-Switching HPLC System for Radiometabolite Analysis. Pharmaceuticals, 2016, 9, 51.	3.8	4
128	Novel PET Radiotracers with Potential Clinical Applications. PET Clinics, 2017, 12, xi-xii.	3.0	4
129	A rapid oneâ€step radiosynthesis of [¹¹ C]â€ <i>d</i> â€ <i>threo</i> â€methylphenidate. Journal of Labelled Compounds and Radiopharmaceuticals, 2011, 54, 168-170.	1.0	3
130	Radionuclide Imaging for Neuroscience: Current Opinion and Future Directions. Molecular Imaging, 2020, 19, 153601212093639.	1.4	3
131	N-Isopropylbenzamide. Acta Crystallographica Section E: Structure Reports Online, 2008, 64, o1005-o1005.	0.2	3
132	Cardiac Sympathetic Positron Emission Tomography Imaging with Meta-[18F]Fluorobenzylguanidine is Sensitive to Uptake-1 in Rats. ACS Chemical Neuroscience, 2021, 12, 4350-4360.	3.5	3
133	Characterization of neuroinflammatory positron emission tomography biomarkers in chronic traumatic encephalopathy. Brain Communications, 2022, 4, fcac019.	3.3	3
134	[11C]-URB694 for FAAH PET imaging: A novel radiotracer for a new target. Neurolmage, 2010, 52, S24.	4.2	2
135	Practical Radiosynthesis and Preclinical Neuroimaging of [11C]isradipine, a Calcium Channel Antagonist. Molecules, 2015, 20, 9550-9559.	3.8	2
136	Aryl- ¹⁸ F Bond Formation from Nucleophilic [¹⁸ F]fluoride. , 2020, , 617-648.		2
137	A New F-18 Labeled PET Agent For Imaging Alzheimer's Plaques. , 2011, , .		1
138	F4-01-04: TAU PET USING F18-T807: INITIAL EXPERIENCE IN NORMAL ELDERLY AND AD DEMENTIA. , 2014, 10, P242-P242.		1
139	Editorial: Positron Emission Tomography (PET) Imaging of Brain Biochemistry: Beyond High-Affinity Radioligands. Frontiers in Neuroscience, 2022, 16, 907460.	2.8	1
140	(E)-2-(2-Methylcyclohexylidene)hydrazinecarbothioamide. Acta Crystallographica Section E: Structure Reports Online, 2011, 67, o3005-o3005.	0.2	0
141	DT-01-02: TEMPORAL NEOCORTICAL TAU DEPOSITION MEASURED WITH PET IS ASSOCIATED WITH LONGITUDINAL DECLINE IN MEMORY PERFORMANCE AMONG CLINICALLY NORMAL ELDERLY. , 2014, 10, P280-P280.		0
142	P2-151: Imaging tau pathology in vivo in ftld with [18F] T807 PET. , 2015, 11, P545-P545.		0
143	Frontispiece: ¹⁸ F‣abeling of Sensitive Biomolecules for Positron Emission Tomography. Chemistry - A European Journal, 2017, 23, .	3.3	0
144	EXTH-49. THERAPEUTIC EFFICACY OF ENGINEERED, HYDROGEL ENCAPSULATED BIMODAL MSC IN GLIOBLASTOMA STRATIFIED ON CELL SURFACE RECEPTOR EXPRESSION. Neuro-Oncology, 2019, 21, vi93-vi93.	1.2	0

#	Article	IF	CITATIONS
145	Repurposing [11C]MC1 for PET Imaging of Cyclooxygenase-2 in Colorectal Cancer Xenograft Mouse Models. Molecular Imaging and Biology, 2021, , 1.	2.6	0
146	PET imaging of glycogen synthase kinase-3 in pancreatic cancer xenograft mouse models American Journal of Nuclear Medicine and Molecular Imaging, 2022, 12, 1-14.	1.0	0